

Flexible semitransparent pentacene thin-film transistors with polymer dielectric layers and NiO_x electrodes

Jiyoul Lee, D. K. Hwang, Jeong-M. Choi, Kimoon Lee, Jae Hoon Kim, and Seongil Im^{a)}
Institute of Physics and Applied Physics, Yonsei University, Seoul 120-749, Korea

Ji Hoon Park and Eugene Kim
Department of Information Display Engineering, Hongik University, Seoul 121-791, Korea

(Received 4 March 2005; accepted 20 June 2005; published online 8 July 2005)

We have fabricated the flexible semitransparent pentacene-based thin-film transistors (TFTs) with poly-4-vinylphenol (PVP) dielectric layers which were deposited by spin coating on a thermostable plastic substrate with a conductive film. For the source/drain (S/D) electrodes of our flexible pentacene TFTs both Au and semitransparent NiO_x have been tested. It was found that NiO_x was better matched to the pentacene channel for the S/D contacts than Au. Our flexible pentacene TFTs with semitransparent NiO_x contacts exhibited mobility of ~ 0.24 cm²/V s higher than that achieved with Au contacts (~ 0.14 cm²/V s) and also demonstrated a higher initial drain current. © 2005 American Institute of Physics. [DOI: 10.1063/1.1996839]

Organic thin-film transistors (OTFTs) have been extensively studied and developed to open the future of organic electronics exemplified by low-end smart cards, drivers for flexible display, and electronic identification tags.¹⁻³ Particularly, pentacene-based OTFTs have already demonstrated their possibilities toward such applications.⁴⁻⁶ Certainly organic thin-film transistors (OTFTs) have key advantages in that they can be fabricated at room temperature even on mechanically flexible plastic substrates. In order to fully exploit these strengths, it is required to successfully obtain suitable polymer dielectric layers on plastic substrates. However, replacing inorganic gate dielectric materials with polymer dielectric layers usually limits the performance of OTFTs because the polymer insulators generally have much lower dielectric capacities than inorganic insulators.^{7,8} Field-effect devices with poly-4-vinylphenol (PVP) appears to have some potentials exhibiting decent mobilities⁹ but those were reported to be still inferior to the devices with inorganic gate oxides in many aspects of device performance. It is thus important and meaningful to find solutions to compensate this drawback of OTFTs with polymer gate dielectric layers.

In the present work, we report on the fabrication and characterization of flexible OTFTs with a pentacene channel, PVP polymer gate insulators, a polyester (PET) substrate coated with a conductive polyethylenedioxythiophene (PEDOT) polymer, and semitransparent NiO_x source/drain (S/D) electrodes that were expected to enhance the source-to-channel injection of hole charges and thus to circumvent the aforementioned drawback of the polymer-gate OTFTs.

Prior to the spin-coating of PVP films on a PEDOT-coated flexible PET substrate (Orgacon™ EL-1500, purchased from Agfa), the surface of the substrate was cleaned with diluted isopropanol for a few seconds. PVP films were then prepared from a solution of PVP and a cross-linking agent (melamine-co-formaldehyde) in propylene glycol monomethyl ether acetate (PGMEA), by spin coating and cross linking (at 175 °C for 30 min. in vacuum). The final thickness of the PVP films was measured to be 450 nm by a

surface profiler (Alpha-Step IQ) while their measured electrical capacitance and leakage current level were ~ 7.4 nF/cm² and $\sim 10^{-7}$ A/cm², respectively.¹⁰ Pentacene channels and S/D pads (NiO_x and Au) were then sequentially patterned on the PVP layer through shadow masks at a substrate temperature of 20 °C [room temperature (RT)] by thermal evaporation in a vacuum chamber with a base pressure of 1×10^{-6} Torr. The deposition rates were fixed to 1 Å/s and 30 Å/s for the pentacene (Aldrich Chem. Co., $\sim 99\%$ purity) and the electrodes, respectively. The thickness of pentacene and electrode films (NiO_x and Au) was 40 and 100 nm, respectively, as monitored by a quartz crystal oscillator and confirmed by the surface profiler. The nominal channel length and width were 90 and 500 μm, respectively. All current-voltage (*I*-*V*) measurements for our OTFTs were performed with a semiconductor parameter analyzer (Agilent 4155C) and the surface of each layer was characterized by atomic force microscopy [(AFM) Nanoscope IV, Digital Instruments].

The photograph in Fig. 1(a) displays our pentacene-based semitransparent OTFT arrays fabricated on a flexible PET substrate and Fig. 1(b) displays the plan view of our TFTs on the emblem of our institute underneath. Even though the source/drain (S/D) electrode regions appear relatively darker than the pentacene channel or PVP layer region, we can nevertheless identify emblem features printed on the paper (see the magnified image of the S/D electrodes). Gen-

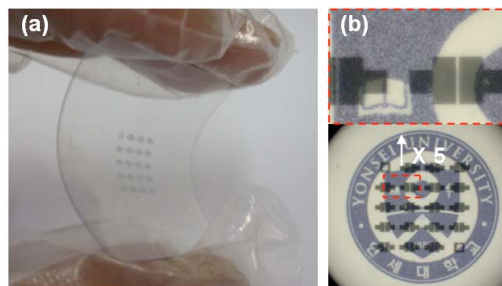


FIG. 1. (Color online) (a) Image of our pentacene-based OTFTs fabricated on a flexible PET substrate; (b) the image plan view of our TFT array on our university emblem underneath.

^{a)} Author to whom correspondence should be addressed; electronic mail: semicon@yonsei.ac.kr

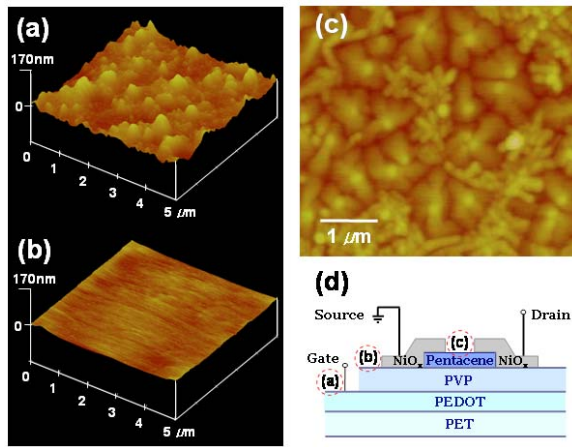


FIG. 2. (Color online) (a) $5 \times 5 \mu\text{m}^2$ AFM image of PEDOT-coated PET substrate as received (b) the surface image of PVP layer coated on the substrate of (a) the surface morphology appeared much improved after deposition; (c) the AFM image of our pentacene film deposited on PVP dielectric film; (d) schematic cross section of our device.

erally, transparent stoichiometric NiO is *p*-type with a band gap of 3.8 eV exhibiting a high transmittance of about 70%.^{11,12} However, our 100-nm-thick NiO_x electrode exhibits a transmittance of only 30% in the visible region but a low sheet resistance of $\sim 60 \Omega/\square$ when it is deposited on Corning glass 7059. Since our NiO_x is probably rather off-stoichiometric and probably in a Ni-rich state as it has been deposited by the thermal evaporation from NiO powder, a somewhat low transmittance is understandable.

The AFM images of each layer of our device are exhibited in Figs. 2(a)–2(c), as indicated in the schematic cross-sectional view of our device in Fig. 2(d). The initial PEDOT on PET substrate showed very rough surface morphology with an rms roughness of 14.68 nm [Fig. 2(a)]. However, the surface roughness has been remarkably improved to 2.61 nm when the PVP dielectric layer was deposited by spin-coating [see Fig. 2(b)]. It is because viscose PVP solutions have filled up the valley regions of the PEDOT surface during the spin coating. The dielectric surface roughness certainly influences the growth of the pentacene channel layer, and our pentacene layers deposited on the smoothed PVP dielectric layer do display relatively well-formed dendritic grains as shown in Fig. 2(c).

Figure 3 shows the drain current-drain voltage (I_D – V_D)

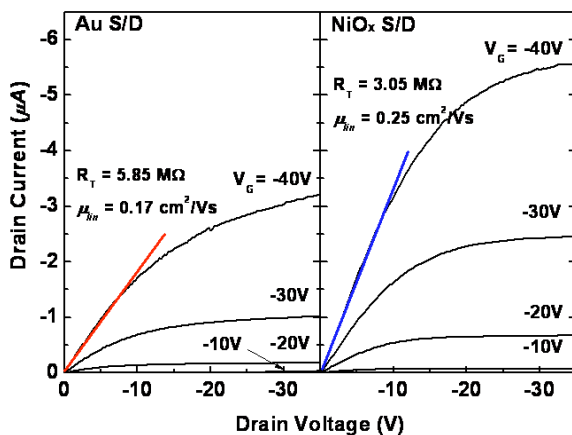


FIG. 3. (Color online) I_D – V_D curves obtained from our flexible TFTs with both Au (left) and NiO_x S/D electrodes (right).

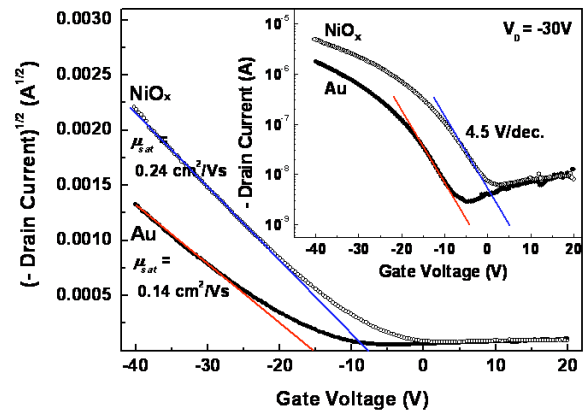


FIG. 4. (Color online) $\sqrt{I_D}$ – V_G curves for the estimation of saturation-regime mobilities that were obtained at $V_D = -30$ V from both OTFTs. The inset plots of $\log_{10}(I_D)$ – V_G show the on/off behavior of our OTFTs.

curves obtained from our pentacene OTFTs fabricated using both metallic Au and NiO_x S/D electrodes. As shown in the figure, the OTFT employing NiO_x S/D electrodes apparently has lower R_T values and a higher saturation current of $\sim 5.5 \mu\text{A}$ under a gate bias (V_G) of -40 V than the other OTFT with Au S/D electrodes that shows the saturation current of only $\sim 3.3 \mu\text{A}$. If we neglect the space-charge-limited current (SCLC) effects, we can consider a total TFT ON-resistance, R_T , in the linear operation regime ($V_D \ll V_G$) as follows:

$$R_T = \frac{V_D}{I_D} = r_{ch}L + 2R_{S/D}, \quad (1)$$

where r_{ch} is the pentacene channel resistance per unit channel-length (L) and $2R_{S/D}$ is the series resistance from both the source and drain contacts.¹³ Since both devices have identical TFT structures and constituent materials except for their electrodes, it is assumed that the r_{ch} values must be the same for both TFTs. This means that the former device with NiO_x has a lower $2R_{S/D}$ value, which is a nominal contact resistance between electrode and channel, and its inversion value now represents a hole-injection efficiency. The injection enhancement effects from NiO_x can also be projected to the drain current behavior with respect to the gate. Using the gradual channel approximation¹⁴ and the Eq. (1) above, we can obtain the total TFT ON-resistance (R_T) from a different formula containing the nominal field-effect mobility and threshold voltage of the OTFT:

$$R_T = \frac{L}{\mu_{lin} C_i W (V_G - V_T)}, \quad (2)$$

where C_i is the gate dielectric capacitance, μ_{lin} the nominal field effect mobility in linear operation regime, V_T the threshold voltage, and W the channel width. According to Fig. 4, the V_T values are measured to be -15 and -7.5 V for the OTFTs with Au and NiO_x S/D contacts, respectively. We thus estimated the nominal mobilities (μ_{lin}) of both OTFTs in the linear regime with V_G of -40 V using Eq. (2), R_T values, and V_T values (extracted from Figs. 3 and 4) Those mobilities were found to be 0.17 and 0.25 $\text{cm}^2/\text{V s}$ for the devices with Au and NiO_x contacts, respectively. [Note that these values should be different from those (μ_{sat}) obtained in the saturation regime ($V_D = -30$ V, see Fig. 4): ~ 0.14 and $\sim 0.24 \text{ cm}^2/\text{V s}$ for the former and the latter, respectively].

It is now interesting to note that the two pentacene channel layers prepared in an identical manner show different mobilities. It is simply because our apparent field mobility includes the electrode-to-channel charge injection process as well as the charge transport within the channel layer. Likewise, based on Eqs. (1) and (2), the S/D contact resistance ($2R_{S/D}$) affects R_T and thus the apparent field-effect mobilities. Due to enhanced charge-injection, our semi-transparent OTFT with NiO_x electrodes does have higher field mobility than the OTFT with Au electrodes. Our NiO_x electrode probably has a larger work function than that of Au (i.e., larger than ~ 5 eV, the work function of Au),¹⁵ consequently being better matched to the pentacene channel. Thermally evaporated at a high deposition rate, semitransparent NiO_x can be in an Ni-rich state so that the Ni-rich oxide may support metallic conduction and also possess the work function properties of metallic Ni (~ 5.15 eV). According to the inset of Fig. 4, both TFTs appeared to have almost the same on/off current ratio of $\sim 10^3$ and subthreshold swing of 4.5 V/dec, which are not very good but moderate for OTFTs using a thin polymer gate dielectric layer.

In summary, we have fabricated flexible semitransparent pentacene-based thin-film transistors with NiO_x S/D electrodes, PVP dielectric, and a PEDOT-coated PET substrate. The pentacene-based TFTs with NiO_x contacts of $\sim 60 \Omega/\square$ exhibited much higher field effect mobility than those with Au contacts because the semitransparent Ni-rich oxide probably has a larger work function than Au thus lowering the contact resistance at the interface between pentacene channel and electrodes (or providing more efficient hole injection into the active channel layers).^{16,17} We thus conclude that using thermally evaporated NiO_x as electrodes is a promising solution to circumvent the current drawback of OTFTs with a low-*k* dielectric polymer gate.

The authors acknowledge the financial support from KISTEP (Program No. M1-0214-00-0228) and the BK 21 Program. J.H.K. acknowledges the support from Yonsei University (Fund No. 1999-1-0029) and eSSC at Postech funded by MOST.

- ¹A. Tsumura, H. Koezuka, and T. Ando, *Appl. Phys. Lett.* **49**, 1210 (1986).
- ²Y. Y. Lin, D. J. Gundlach, S. F. Nelson, and T. N. Jackson, *IEEE Trans. Electron Devices* **44**, 1325 (1997).
- ³C. D. Dimitrakopoulos and P. R. L. Malenfant, *Adv. Mater. (Weinheim, Ger.)* **14**, 99 (2002).
- ⁴P. F. Baude, D. A. Ender, M. A. Hasse, T. W. Kelly, D. V. Muires, and S. D. Theiss, *Appl. Phys. Lett.* **82**, 3964 (2003).
- ⁵M. Kitamura, T. Imada, and Y. Arakawa, *Appl. Phys. Lett.* **83**, 3410 (2003).
- ⁶H. Klauk, M. Halik, U. Zschieschang, F. Eder, G. Schmid, and C. Dehm, *Appl. Phys. Lett.* **82**, 4175 (2003).
- ⁷M. Halik, H. Klauk, U. Zschieschang, G. Schmid, W. Radlik, and W. Weber, *Adv. Mater. (Weinheim, Ger.)* **14**, 1717 (2002).
- ⁸J. Veres, S. Ogier, G. Lloyd, and D. de Leeuw, *Chem. Mater.* **16**, 4543 (2004).
- ⁹H. Y. Choi, S. H. Kim, and J. Jang, *Adv. Mater. (Weinheim, Ger.)* **16**, 732 (2004).
- ¹⁰D. K. Hwang, J. H. Park, J. Lee, J.-M. Choi, J. H. Kim, E. Kim, and S. Im, *Electrochem. Solid-State Lett.* **8**, G140 (2005).
- ¹¹G. A. Sawatzky and J. W. Allen, *Phys. Rev. Lett.* **53**, 2339 (1984).
- ¹²H. Ohta, M. Hirano, K. Nakahara, H. Maruta, T. Tanabe, M. Kamiya, T. Kamiya, and H. Hosono, *Appl. Phys. Lett.* **83**, 1029 (2003).
- ¹³S. Luan and G. W. Neudeck, *Appl. Phys. Lett.* **72**, 766 (1992).
- ¹⁴S. M. Sze, *Physics of Semiconductor Devices*, 2nd ed. (John Wiley, New York, 1981), pp. 438–445.
- ¹⁵G. Wakefield, P. J. Dobson, Y. Y. Foo, A. Loni, A. Simons, and J. L. Hutchison, *Semicond. Sci. Technol.* **12**, 1304 (1997).
- ¹⁶H. Sirringhaus, T. Kawase, R. H. Friend, T. Shimoda, M. Inbasekaran, W. Wu, and E. P. Woo, *Science* **290**, 2123 (2000).
- ¹⁷N. Koch, A. Elschner, J. Schwartz, and A. Kahn, *Appl. Phys. Lett.* **82**, 2281 (2003).